

Solute redistribution in a duplex dendritic structure

G. W. SWARTZBECK

Westinghouse Electric Corporation, Pittsburgh, Pennsylvania, USA

T. Z. KATTAMIS

Department of Metallurgy, Institute of Materials Science, University of Connecticut, Storrs, Connecticut, USA

A duplex dendritic structure consists of co-existing regions of coarse and fine dendrites. Such a structure in aluminium-4.5 wt % copper alloy was produced by rapid quenching from the partially solid-partially liquid state. The concentration of solute was found to be low and constant within the coarse structure, which contains a smaller amount of non-equilibrium secondary phase than does the fine dendritic structure. The solute distribution profiles within both the coarse and fine dendritic structures were found to be fairly accurately described by the Scheil equation for non-equilibrium solidification. Complete dissolution of the secondary phase occurred within the coarse structure after a shorter solutionizing time than it did within the fine dendritic structure. A spherical diffusion model accurately described solution kinetics within the coarse structure and a cylindrical diffusion model within the fine structure.

1. Introduction

The solidification of an alloy cast in the solid-liquid range takes place in two stages: during the first stage the solid nucleates and grows slowly in the crucible or the ladle; during the second stage growth continues in the mould at a higher rate. The resulting microstructure is "duplex", consisting of coarse dendrites embedded in a finer fern-like dendritic matrix [1]. Such microstructures are frequently observed in continuously-cast and die-cast alloys. Thus Fig. 11-(3) of [2] and Fig. 4 of [3] exhibit duplex structures in continuously-cast aluminium alloys and Fig. 1 of [4] exhibits duplex structures in die-cast alloy steel. Duplex structures are also obtained in "rheocast" alloys [5, 6]. In this process, alloys are vigorously agitated during the early stages of solidification and behave as thixotropic mixtures of liquid and solid that are highly fluid up to a fraction solid of 0.40 and can be cast or die-cast.

Certain structural peculiarities previously observed and described are basically duplex structures. Thus, Southin [7] observed that

grains in the equiaxed zone of cast aluminium and aluminium-copper alloy ingots containing up to 2 wt % copper had a "comet" shape with a coarse dendritic head and a fine dendritic tail which was part of the surrounding columnar structure. His experiments indicated that dendritic particles shower from the surface layer of the ingot and become the heads of the comet grains. A similar structure was reported by Chalmers *et al* [8]. Cole *et al* [9], studying the effect of fluid motion on ingot solidification of aluminium-copper alloys containing up to 2 wt % copper, observed the existence of special equiaxed grains which had rounded sides, radiated from a central symmetrical core and exhibited no dendritic geometry. With increasing solute concentration the number of these grains increased and an internal substructure gradually developed. These authors [9] assumed that these new grains grew from dendrite arms which were detached from the growing interface by the intense fluid flow generated through oscillatory motion.

The present investigation was undertaken to

develop a better understanding of the establishment of duplex dendritic structure and of the redistribution of solute in such a structure during solidification and during a solution treatment.

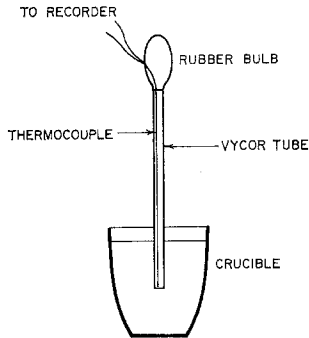


Figure 1 Schematic representation of the experimental setup.

2. Experimental procedure

2.1. Melting and casting

Basically two different procedures were followed for specimen preparation: in the first procedure the alloy was melted in a clay-graphite crucible coated with zircon wash, using standard melting procedure. The temperature was decreased to below the liquidus and the system was stirred vigorously for 1 to 2 min in order to homogenize the solid plus liquid mixture (slurry). The slurry was drawn up at various temperatures into a 0.5 in. i.d. vycor glass tube by release of a squeezed rubber bulb, Fig. 1. The tube was subsequently removed quickly and air-cooled. Temperature was recorded using a fine chromel-alumel thermocouple protected in an alumina sheath. The thermocouple wires passed through a hole in the bulb sealed with rubber cement. For slurries containing more than 30% solid a slightly different procedure was adopted: The solid + liquid slurry was vigorously stirred just below the liquidus temperature and the vycor glass tube introduced in it without the rubber bulb. The alloy was gradually cooled down and at the appropriate temperature the rubber bulb was squeezed, placed at the end of the tube and released. The tube was removed quickly and allowed to air cool. In all the runs made, approximately the same amount of metal was drawn into the tubes from the same position in the crucible. Alloys used in this investigation were: aluminium-4.5 wt % copper, aluminium-

20 wt % copper and grain-refined aluminium-4.5 wt % copper-0.2 wt % titanium.

2.2. Specimen preparation and examination

Specimens were polished and etched with Keller's reagent. Measurements of the volume fraction of secondary phase were made by quantitative metallography using a two-dimensional systematic point count [10, 11]. In each analysis, 4000 to 5000 points were applied with a 16-point grid inscribed on a reticule in the eyepiece of the metallograph. The fraction of points falling over each phase represented the volume fraction of the particular phase. The volume fraction of the coarse dendritic structure was measured using lineal and areal analyses [12, 13].

Successive polishing of the specimens in the as-cast condition revealed that the coarse microstructure consists of dendrite "cells" which are isometric, almost spherical. Cell size measurements were carried out by making many random traverses across photomicrographs of the sample and counting the number of cells intercepted by the lines. The mean lineal intercept was then obtained from:

$$\bar{L} = 1/N$$

where \bar{L} is the average lineal intercept in three dimensions and N is the number of cells intersected per unit length of line. From a simple statistical analysis the average cell size in three dimensions was then taken as approximately equal to [14, 15]:

$$\bar{D} = 1.5\bar{L}$$

where \bar{D} is the average grain diameter.

Several slices were taken from plates which had been cast below the liquidus temperature in order to study the solution kinetics of the non-equilibrium interdendritic secondary phase. The solution treatment was conducted at 535°C for times up to 8 h and was followed by warm (40°C) water quench.

The distribution of copper across the coarse and fine dendritic structures was established using an A.R.L. No. 21000 electron microprobe with a take-off angle of 52.5°. In a few instances the electron beam was defocused in order to measure average copper concentrations.

3. Results and discussion

3.1. Dendritic microstructure

The microstructure of aluminium-4.5 wt % copper alloy cast at various temperatures

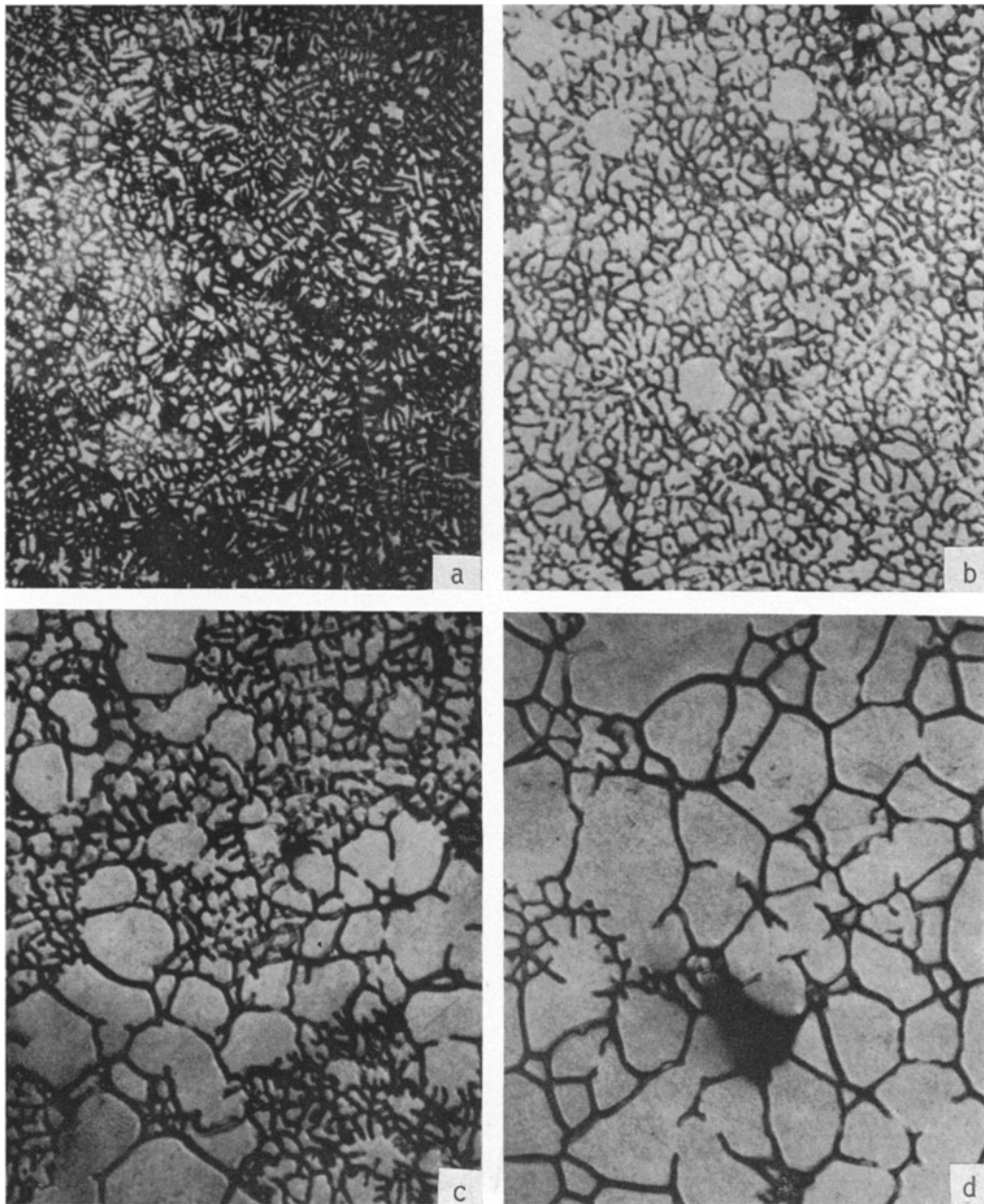


Figure 2 Photomicrographs of Al-4.5 wt% Cu alloy specimens cast at various temperatures below the liquidus (646°C) and cooled at approximately $37^{\circ}\text{C min}^{-1}$ ($\times 50$). Casting temperatures were: (a) 647°C , (b) 645°C , (c) 643°C and (d) 625°C .

below the liquidus consists of a coarse dendritic structure embedded in a fine dendritic structure, Fig. 2b to d. The coarse structure is an agglomerate of large dendrite cells [1] sometimes reduced to isolated spheroids. The volume

fraction of this coarse structure was found to increase with decreasing casting temperature, as illustrated in Fig. 3. Recorded cooling curves are given in Fig. 4 for specimens cast at 692 , 640 and 635°C and for a specimen solidified

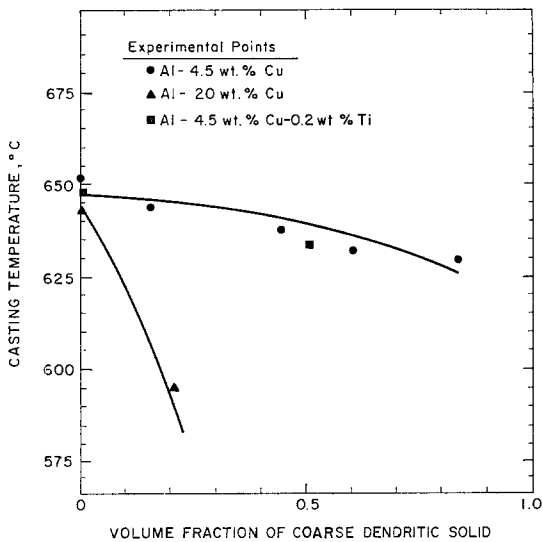


Figure 3 Relationship between casting temperature and volume fraction of coarse dendritic solid. Curves derived using the Scheil equation for Al-4.5 wt % Cu and Al-20 wt % Cu.

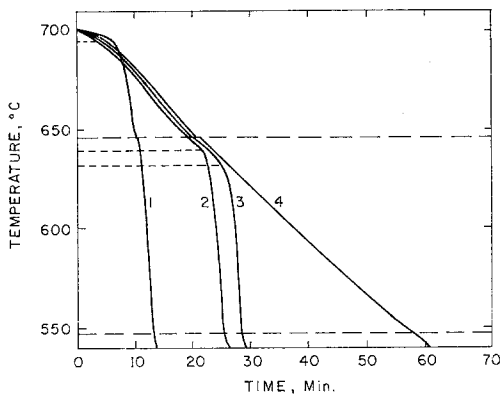


Figure 4 Cooling curves of Al-4.5 wt % Cu alloy specimens cast at various temperatures. (1) 692°C, (2) 640°C, (3) 635°C, (4) specimen solidified in the crucible.

completely in the crucible. In a first series of experiments, the average cooling rate of the metal in the crucible was approximately $2.8^{\circ}\text{C min}^{-1}$ and in the vycor tube, $37^{\circ}\text{C min}^{-1}$; in a second series of experiments these rates were $1.1^{\circ}\text{C min}^{-1}$ and $37^{\circ}\text{C min}^{-1}$, respectively. The coarse dendritic structure resulted from growth of the solid in the crucible and later on in the tube. Coarsening and coalescence [1] seem to have played an important role in the establishment of final microstructure. It is believed that coarsening was accelerated by the

relative motion of liquid and solid [16] during stirring of the mixture in the crucible and during filling of the tubes.

Analogous observations were made on duplex structures in aluminium-20 wt % copper alloy, Fig. 5a and b. However, in this alloy the coarse structure exhibits more definite dendritic features than in the aluminium-4.5 wt % copper alloy. This could be attributed to the decrease in coarsening rate with increasing solute concentration [1]. Similarly, in the duplex structure of aluminium-4.5 wt %-0.2 wt % titanium grain-refined alloy, Fig. 5c and d, the grains in the coarse structure are equiaxed dendritic, possibly because coarsening and coalescence were slowed down by a decrease in the solid-liquid interface energy caused by the addition of titanium.

The volume fraction of coarse structure versus temperature at which the alloy was cast is plotted in Fig. 3 for aluminium-4.5 wt % copper alloy. Upon converting to weight fractions the non-equilibrium solidification equation was found to accurately predict the amount of coarse dendritic solid.

3.2. Redistribution of solute

The distribution of copper within the coarse and fine dendritic structures in an aluminium-4.5 wt % copper alloy specimen cast 1.5°C below the liquidus temperature was first investigated by defocusing the beam of the electron microprobe. Fig. 6 shows that inside the coarse structure the average copper concentration is about 1 wt %, whereas across the fine dendritic structure it is about 5 wt %. Typical distribution profiles established with focused beam using $2\ \mu\text{m}$ steps are illustrated in Fig. 7. The profile XY inside a spherical particle of the coarse structure exhibits a plateau at about 1 wt % copper. The concentration rises to about 53 wt % copper at points X and Y which fall within Al_2Cu regions. The distribution profile UV across a dendrite arm of the fine dendritic structure exhibits a narrow minimum at about 2 wt % copper. Along path ZW the corresponding minimum concentration is about 3 wt % copper, presumably because the plane of polish did not pass through the axis of the dendrite arm.

The volume fraction of non-equilibrium interdendritic eutectic was measured and found to be about 0.065 in the fine dendritic structure and 0.025 in the coarse structure.

Typical distribution profiles of copper across

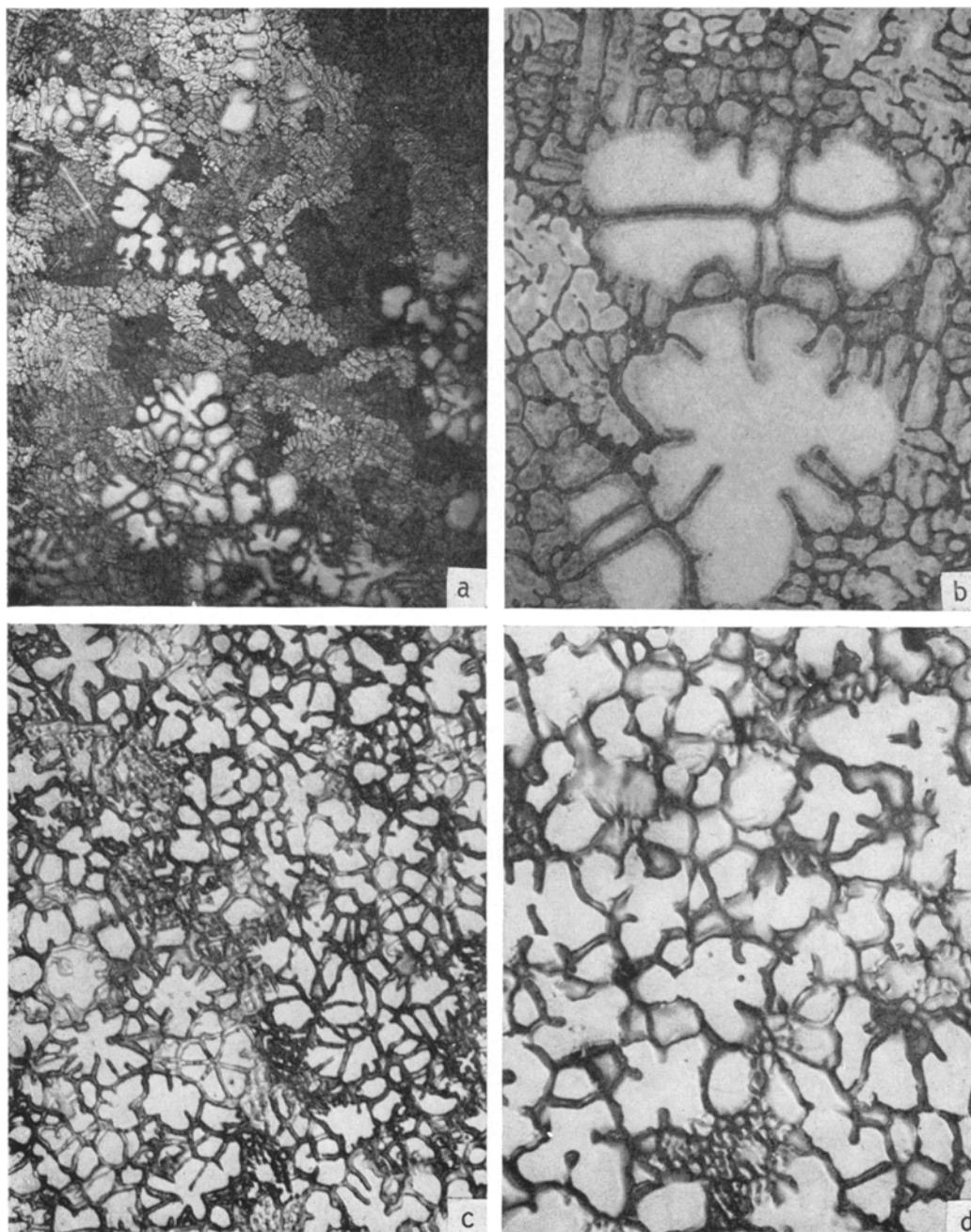


Figure 5 Photomicrographs of duplex dendritic structure. Al-20 wt % Cu alloy specimens cast at 589°C, 3°C below the liquidus and cooled at 28°C min⁻¹. (a) ×25, (b)×70. Al-4.5 wt % Cu-0.2 wt % Ti alloy specimens cast at 634°C, 12°C below the liquidus and cooled at 35°C min⁻¹. (c) ×35, (d) ×60.

the coarse and fine dendritic structures were replotted in Fig. 8a and b versus r/a and r/a' , respectively. The coarse structure was assumed to consist of an agglomerate of spherical cells

of radii, a , and the fine structure of cylindrical arms of radii a' ; r is current distance from the centre of the sphere or the axis of the cylinder. For comparison the Scheil concentration dis-

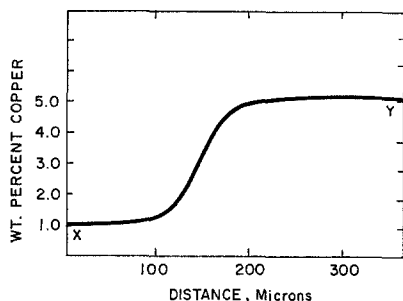
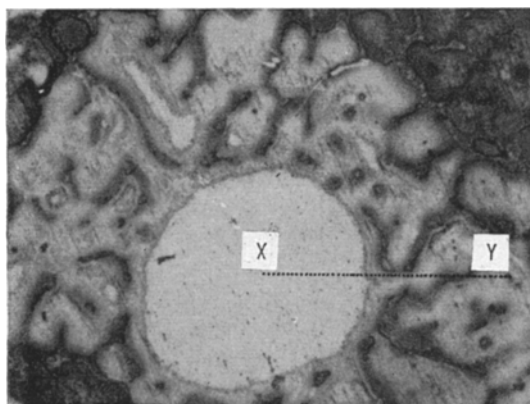


Figure 6 Distribution of copper along path XY shown in photomicrograph. Al-4.5 wt % Cu alloy specimen cast at 640°C. Defocused electron beam.

tribution in the solid has been plotted in the two cases assuming constant partition ratio, no diffusion in the solid and complete diffusion in the liquid. For the coarse structure, the "volume element" [17] size or final cell radius was determined assuming that the melt was allowed to solidify completely in the crucible at $1.1^\circ\text{C min}^{-1}$. Local solidification time would then be 6.5×10^3 sec and average cell diameter [18] would be approximately 230 μm instead of 140 μm , the actual measured average cell diameter.

At 1.5°C below the liquidus temperature, the weight fraction solid predicted by the Scheil equation is 0.15 and the copper concentration at the solid-liquid interface $C_s = 0.9$ wt %. This weight fraction solid corresponds to a cell radius of approximately 59 μm at the time of quench. The curve between 0.15 and 1.00 ($r = 59$ μm and $r = 70$ μm , respectively) has been plotted using again the Scheil equation with an average copper concentration $C_0 = 4.9$ wt % and a volume element of radius 11 μm . This concentration was calculated by mass balance, assuming that a weight fraction solid of 0.15 and average concentration 0.9 wt % forms at

1.5°C below the liquidus temperature before quenching, and is in close agreement with experimental results obtained using a defocused electron beam, Fig. 6. The predicted solute distribution, Fig. 8a, is in good agreement with the electron microprobe results.

The role of coarsening in the establishment of the morphology of the coarse dendritic structure has been explained above. It is believed that coarsening plays an important role in the redistribution of solute within the coarse dendritic structure. On the other hand back-diffusion of solute in the solid during and after solidification is expected to have been of little importance, mainly because of the large spacings or diffusion distances involved. Finally, for individual spherical crystals drifting in the melt a steady-state growth could be postulated. Such a growth would then explain the observed concentration plateau [19]. For the fine dendritic structure it was assumed that the initial copper

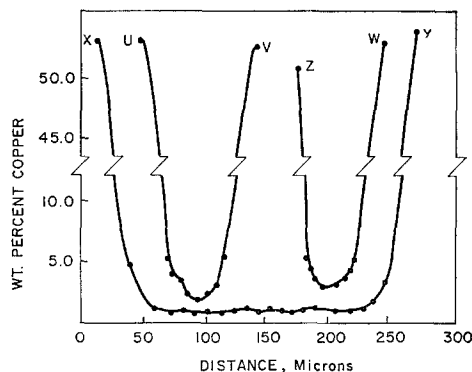
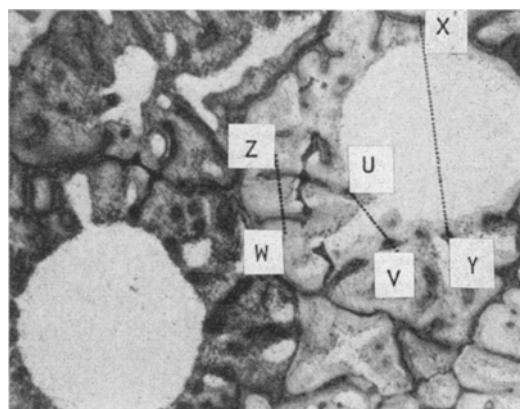


Figure 7 Distribution of copper along three paths: XY, UV and ZW shown in the photomicrograph. Al-4.5 wt % Cu alloy specimens cast at 640°C. Focused electron beam.

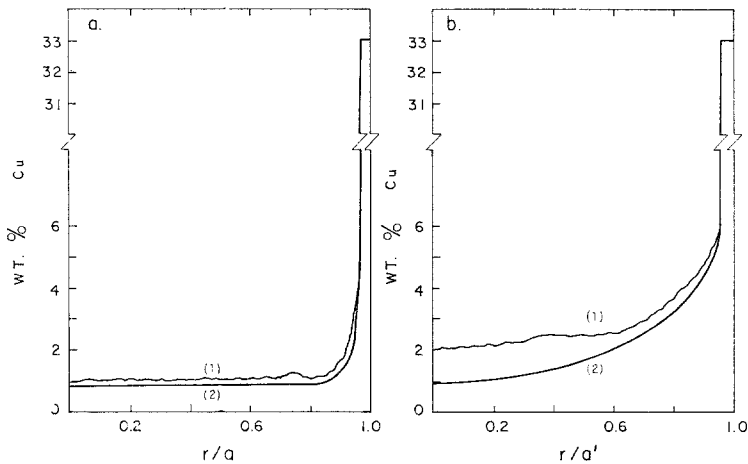


Figure 8 (a) Solid composition versus distance across a coarse dendrite cell. (1) Experimental curve, (2) theoretical curve; (b) solid composition versus distance across a fine dendrite arm. (1) Experimental curve, (2) theoretical curve.

concentration was 4.9 wt % copper and that the volume element was cylindrical of radius 25 μm . Calculated and experimental copper distribution profiles for the fine dendritic structure are illustrated in Fig. 8b. The observed discrepancy could be attributed to back-diffusion of copper in the solid, a process which appears possible for spacings of about 25 μm . The reasonable validity of the Scheil equation was also tested by comparing predicted and measured volume fractions of eutectic in the coarse and fine dendritic structures. Thus, in the coarse structure the predicted volume fraction eutectic was 0.0220 and that measured was 0.25, whereas in the fine structure they were 0.062 and 0.065, respectively.

3.3. Solution kinetics

The non-equilibrium secondary phase in the coarse structure disappeared faster than in the fine dendritic structure, Figs. 9 and 10. In the as-cast condition, the volume fraction of secondary phase in the coarse structure was 0.025 and in the fine structure 0.065. After a 4 h solution treatment at 535°C, the secondary phase dissolved completely in the coarse structure, whereas about 25% remained undissolved in the fine structure.

After completion of dissolution of the secondary phase in the coarse structure, a substantial amount of coring remained within the dendrite cells, Fig. 9a, as confirmed by electron probe microanalysis.

The higher dissolution rate of secondary

phase observed in the coarse structure, Fig. 9, is rather paradoxical [20, 21] because diffusion distance for this structure is longer than for the fine structure. An explanation for this could be based on geometrical differences between the coarse dendrite cells, which may be assumed spherical, and the fine dendrite arms, which may be assumed cylindrical. It could also be based on the difference in solute distributions within these geometries, in particular the steep concentration gradient in the solid at the interface between primary and secondary phases. In the coarse structure this gradient is 1.2×10^4 wt % Cu cm^{-1} , as opposed to 6×10^3 wt % Cu cm^{-1} in the fine. Two models were developed to describe solution kinetics: a spherical diffusion model for the coarse structure and a cylindrical diffusion model for the fine structure [22]. Other assumptions made were:

1. the initial solute concentration is constant and equal to 1 wt % copper inside the sphere, rising to 5.3 wt % copper at the surface of the sphere. Inside the cylinder, copper is initially distributed as predicted by the non-equilibrium solidification equation;
2. the surface concentration $C_M = 5.3$ wt % copper, the solvus concentration at 535°C;
3. the secondary phase is continuous around the sphere or the cylinder;
4. the boundary between primary and secondary phases is immobile during the solution treatment. This simplification can be justified by the very small thickness of the secondary phase. More elaborate models account for the

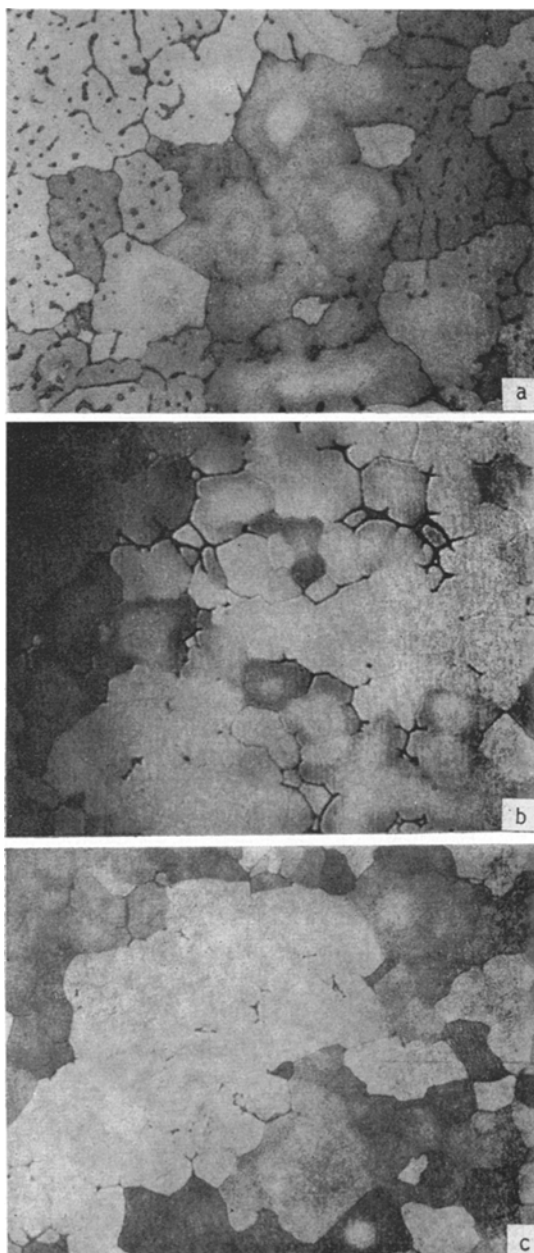


Figure 9 Photomicrographs of cast Al-4.5 wt % Cu alloy solutionized at 535°C for (a) 1 h, (b) 3 h and (c) 8 h.

boundary movement [23].

Other details and derivation, using this model, of a relation between g/g_0 and solutionizing time, where g = volume fraction of secondary phase remaining after dissolution for time t and g_0 = initial volume fraction of secondary phase, were previously described [22]. Fig. 10

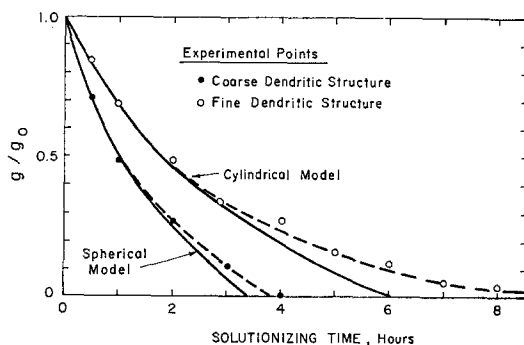


Figure 10 Relative amount of secondary phase remaining after a given solutionizing time. Specimens solutionized at 535°C.

compares analytical curves for the spherical and cylindrical diffusion models with experimental curves established for the coarse and fine dendritic structures, respectively, using a systematic point count of secondary phase.

In general, the adopted models describe fairly accurately the dissolution processes in the corresponding structures. The observed discrepancy for longer solutionizing times could be attributed to a finite amount of secondary phase being located between primary dendrite arms rather than secondary arms, with corresponding longer diffusion distances, and to the discontinuity of secondary phase which would increase the solutionizing time.

4. Conclusions

1. Co-existing regions of coarse dendrite cells and fine dendrites may form by quenching a liquid plus solid mixture.

2. The concentration of solute is low and constant within the coarse structure. The distribution of solute within both the coarse and the fine dendritic structures is fairly accurately described by the Scheil equation.

3. A larger amount of non-equilibrium secondary phase is associated with the fine dendritic structure than with the coarse.

4. Complete dissolution of the non-equilibrium secondary phase occurred within the coarse structure after a shorter solutionizing time than it did within the fine dendritic structure.

5. A spherical diffusion model accurately described solution kinetics within the coarse structure and a cylindrical diffusion model within the fine structure.

Acknowledgement

This work was sponsored by a University of Connecticut Research Foundation Grant.

References

1. K. H. CHIEN and T. Z. KATTAMIS, *Z. Metallk.* **61** (1970) 475.
2. D. ALTENPOHL, R. C. FORNEROD and A. STEINER, *ibid* **60** (1969) 576.
3. G. MORITZ, *ibid* **60** (1969) 694.
4. D. T. HURD, R. L. BERTO and J. P. SOLTENBERG, *Trans. A.F.S.* **99** (1968) 511.
5. D. B. SPENCER, R. MEHRABIAN and M. C. FLEMINGS, *Met. Trans.* **3** (1972) 1925.
6. R. MEHRABIAN and M. C. FLEMINGS, accepted for publication, *Trans. A.F.S.*
7. R. T. SOUTHIN, *Trans. Met. Soc. AIME* **239** (1967) 220.
8. H. BILONI and B. CHALMERS, *ibid* **223** (1965) 373.
9. G. S. COLE and G. F. BOLLING, "The Solidification of Metals" (Iron and Steel Institute, Publication 110, London, 1967) p. 323.
10. J. E. HILLIARD and J. W. CAHN, *Trans. Met. Soc. AIME* **221** (1961) 344.
11. A. K. BHAMBRI and T. Z. KATTAMIS, *Met. Trans.* **2** (1971) 1869.
12. R. T. DEHOFF and F. N. RHINES, "Quantitative Microscopy" (McGraw-Hill, New York, 1968).
13. E. E. UNDERWOOD, "Quantitative Stereology" (Addison Wesley, Reading, Mass., 1970).
14. C. S. SMITH and L. GUTTMAN, *Trans. Met. Soc. AIME* **197** (1953) 81.
15. R. L. FULLMAN, *ibid* **197** (1953) 447.
16. T. Z. KATTAMIS, current investigation, Department of Metallurgy, University of Connecticut, Storrs, Connecticut.
17. H. D. BRODY and M. C. FLEMINGS, *Trans. Met. Soc. AIME* **236** (1966) 615.
18. T. Z. KATTAMIS, J. C. COUGHLIN and M. C. FLEMINGS, *ibid* **239** (1967) 1504.
19. D. A. MELFORD and D. A. GRANGER, "The Solidification of Metals" (Iron and Steel Institute, Publication 110, London, 1967) p. 289.
20. S. N. SINGH and M. C. FLEMINGS, *Trans. Met. Soc. AIME* **245** (1969) 1803.
21. K. H. CHIEN, T. Z. KATTAMIS and F. R. MOLLARD, *Met. Trans.* **4** (1973) 1069.
22. G. W. SWARTZBECK and T. Z. KATTAMIS, *Z. Metallk.* **63** (1972) 295.
23. R. A. TANZILLI and R. W. HECKEL, *Trans. Met. Soc. AIME* **242** (1968) 2313.

Received 3 July and accepted 17 September 1973.